Solid-State Electronics Vol. 23, pp. 209–216
Pergamon Press Ltd., 1980. Printed in Great Britain

THE OPEN-CIRCUIT VOLTAGE OF BACK-SURFACE-FIELD (BSF) *p–n* JUNCTION SOLAR CELLS IN CONCENTRATED SUNLIGHT†

CHING-YUAN WU and WEN-ZEN SHEN

Semiconductor Research Center and Institute of Electronics, National Chiao-Tung University, Hsin-Chu, Taiwan, Republic of China

(*Received* 18 *June* 1979; *in revised form* 1 *September* 1979)

Abstract—Simple analytical expressions for the open-circuit voltage of the n^+–p–p^+ and p^+–n–n^+ BSF solar cells, which are valid for both the low- and high-levels of optical illumination, are derived. Based on the principle of superposition the open-circuit voltage of both the n^+–p–p^+ and p^+–n–n^+ solar cells are expressed in terms of the short-circuit current and the known saturated dark current. Effects of the high-low junction doping, the energy-gap shrinkage, and the dimensions of the BSF solar cells on the open-circuit voltage are included. The numerical results of the derived expressions are found to be in good agreement with the exact numerical analysis of Fossum *et al.* The optimal design considerations based on the known characteristics of the open-circuit voltage are also discussed.

1. INTRODUCTION

The behavior of back-surface-field (BSF) solar cells in concentrated sunlight is of both scientific and economic interest. From the scientific point of view, it is of interest to understand both the internal physical processes and the external performance parameters as the illumination level is increased. From the economic point of view, the increases of the solar cell efficiency and output power under high-level illumination, can replace the existing expensive solar cell area with equivalent areas of lower-cost refractive or reflective materials, which make both single-crystal silicon and gallium arsenide solar cells possible of being considered for applications in low-cost terrestrial photovoltaic system. The principal merits of BSF solar cells are high open-circuit voltage, high short-circuit current, and high power conversion efficiency when comparing with those of the conventional p–n junction solar cells. The origin of these dramatic improvements comes from the advent of the high-low junction which tends to suppress the minority-carrier current injected from the near-by p–n junction. Godlewski *et al.*[1] had analyzed the performance of such cells under low-level injection conditions. Sabnis[2] had extended the work of Godlewski *et al.* to include high-levels of injection using the ambipolar diffusion equation developed by Dhariwal *et al.*[3], but their developed equations are in term of uniform generation rate. Recently, Fossum *et al.*[4] have used the exact numerical analysis to simulate the physical behaviors of BSF solar cells in concentrated sunlight (from 1 to 500 suns). Due to the needs of longer computer time, Fossum *et al.* have also developed the analytical expressions for the open-circuit voltage of the n^+–p–p^+ and p^+–n–n^+ back-surface-field solar cells. However, disagreements between the analytical expressions and the results of the exact numerical analysis are apparent, especially, for the low- and medium-levels of optical illumination. Moreover, no detailed presentations of their analytical calculations and the enough data of their exact computer analysis are given in their published papers[4, 5].

In this paper, detailed calculations based on more realistic assumptions and boundary conditions are presented. The analytical expressions for the open-circuit voltage of the n^+–p–p^+ and p^+–n–n^+ solar cells in concentrated sunlight are derived. Based on the principle of superposition the open-circuit voltages of both the n^+–p–p^+ and p^+–n–n^+ solar cells are expressed in terms of the short-circuit current and the saturated dark current of the dark diode. It is found that the derived analytical expressions are in good agreement with the exact computer-aided numerical analysis of Fossum *et al.* Moreover, the optimal design considerations based on the open-circuit voltage of the BSF solar cell are also discussed.

2. BASE REGION VOLTAGE AND HIGH-LOW JUNCTION VOLTAGE

Consider a p^+–n–n^+ solar cell, as shown in Fig. 1, in which the emitter is thin (~0.25 μm) and heavily doped ($N_{AE} \sim 10^{20}$/cm^3), the low concentration base region is thick (150 μm ~ 300 μm) and lightly doped with reasonably long minority carrier diffusion length, the high-concentration base region is thin (0.5 ~ 5 μm) and heavily doped ($N_{Dh} \sim 10^{19}$/cm^3). The electrical behavior

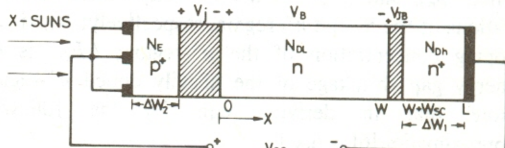

Fig. 1. Typical p^+–n–n^+ solar cell structure illustrating the components and polarities of the open-circuit voltage V_{oc}.

†This research was supported by National Sciences Council, Rep. of China under the contract NSC-68E-0404(02)

of this cell can be adequately described by physical mechanisms occuring in the neutral-base region. The basic equations used to characterize the solar cell parameters are the current flow equations and the continuity equations for electrons and holes:

$$J_n(x) = q\mu_n n(x)\epsilon(x) + qD_n \frac{\partial n}{\partial x} \quad (1)$$

$$J_p(x) = q\mu_p p(x)\epsilon(x) - qD_p \frac{\partial p}{\partial x} \quad (2)$$

$$\frac{\partial n(x)}{\partial t} = \frac{1}{q}\frac{\partial J_n(x)}{\partial x} + G_n - U_n = 0 \quad (3)$$

$$\frac{\partial p(x)}{\partial t} = -\frac{1}{q}\frac{\partial J_p(x)}{\partial x} + G_p - U_p = 0 \quad (4)$$

where G_n, G_p are optical generation rates for electrons and holes, respectively; U_n, U_p are recombination rates for electrons and holes, respectively.

To derive an expression for quasi-neutral base region voltage V_B under the open-circuit condition, the built-in electric field in the neutral-base region must be calculated. Under the open-circuit condition, the built-in electric field may be easily obtained by combining eqns (1) and (2) with the constraint of zero total current, $J_t = J_n(x) + J_p(x) = 0$:

$$\epsilon(x) = \frac{D_p \frac{\partial p}{\partial x} - D_n \frac{\partial n}{\partial x}}{\mu_n n(x) + \mu_p p(x)}. \quad (5)$$

Using the charge neutrality condition in the low concentration base region, $n_n(x) = p_n(x) + N_{Dl}(x)$, the quasi neutral-base region voltage V_B may be obtained by integrating eqn (5) across the low concentration base region, which yields:

$$V_B = \frac{k_BT}{q}\left(\frac{b-1}{b+1}\right)\ln\left\{\frac{p_n(0) + \frac{bN_{Dl}}{b+1}}{p_n(w) + \frac{bN_{Dl}}{b+1}}\right\} \text{ for } p^+\text{-}n\text{-}n^+ \quad (6)$$

where $b = (\mu_n/\mu_p) = (D_n/D_p)$; $p_n(0)$ and $p_n(w)$ are the minority carrier concentrations at the edges of the low impurity concentration neutral-base region, and are the function of optical illumination.

The built-in voltage of the high-low junction at thermal equilibrium condition, V_{hl0}, can be written as

$$V_{hl0} = \frac{k_BT}{q}\ln\left(\frac{p_{n,0}}{p^+_{n,0}}\right) = \frac{k_BT}{q}\ln\left(\frac{N_{Dh}}{N_{Dl}}\right) - \frac{\Delta E_{G1}}{q} \quad (7)$$

where $p_{n,0}$ and $p^+_{n,0}$ are the minority carrier concentrations of the n- and n^+-region, respectively; N_{Dh} is the doping concentration of the n^+-region; ΔE_{G1} is the energy gap shrinkage of the heavily doped n^+-region. Note that in deriving eqn (7) the following approximation[6] is used:

$$n^2_{ih} = n^2_{io}\exp\left(\frac{\Delta E_{G1}}{k_BT}\right) \quad (8)$$

where n_{io} is the intrinsic carrier concentration of lo[w] impurity concentration; n_{ih} is the intrinsic carrier con[-]centration of high impurity concentration.

The built-in voltage of the high-low junction und[er] optical illumination, V_{hl}, can also be written as

$$V_{hl} = \frac{k_BT}{q}\ln\left(\frac{p_n(w)}{p_n^+(w + w_{sc})}\right) \quad (9)$$

where $p_n(w)$ and $p_n^+(w + w_{sc})$ are the minority carri[er] concentrations at the edges of the low-high juncti[on] under optical illumination, respectively. Using the charg[e] neutrality relation, $n_n(w) = p_n(w) + N_{Dl}$, the np produ[ct] relation at the edges of the high-low junction can b[e] written as

$$p_n(w)[N_{Dl} + p_n(w)] = p_n^+(w + w_{sc})N_{Dh}\exp\left(-\frac{\Delta E_{G1}}{k_BT}\right) \quad (10)$$

Using eqns (7), (9) and (10) the change of the built-i[n] voltage under optical illumination can be easily cal[-]culated and written as

$$V_{jB} = V_{hl0} - V_{hl} = \frac{k_BT}{q}\ln\left[1 + \frac{p_n(w)}{N_{Dl}}\right] \text{ for } p^+\text{-}n\text{-}n^+ \quad (11)$$

where $p_n(w)$ is also a function of optical illuminatio[n]. For example, at low illumination level, $p_n(w) \ll N_{Dl}$, V_{jB} is approximately equal to zero, which means that th[e] contribution of the high-low junction voltage to extern[al] open-circuit voltage is zero. Note that all equatio[ns] derived above are quite exact, and satisfy for both th[e] low- and high-levels of optical illumination.

To relate the minority carrier concentration at $X = w$, $p_n(w)$, to $p_n(0)$, the following equation is used, whi[ch] may be calculated by solving the current flow equatio[n] and the continuity equation (see Appendix):

$$p_n(w) \cong \frac{p_n(0)}{\cosh\left(\frac{w}{L'_{pl}}\right) + \frac{S_{nn^+}L'_{pl}}{D'_{pl}}\sinh\left(\frac{w}{L'_{pl}}\right)} \quad (12)$$

where L'_{pl} and D'_{pl} are the effective minority carri[er] diffusion length and diffusivity in the low concentrati[on] base region under optical illumination; S_{nn^+} is th[e] recombination velocity of the minority carrier at th[e] n–n^+ junction under optical illumination, which may b[e] written as (see appendix):

$$S_{nn^+} = S^0_{nn^+}\left[1 + \frac{p_n(w)}{N_{Dl}}\right] \quad (13)$$

$$S^0_{nn^+} = \frac{N_{Dl}D_{ph}}{N_{Dh}L_{ph}}\exp\left(\frac{\Delta E_{G1}}{k_BT}\right)\coth\left(\frac{\Delta w_1}{L_{ph}}\right) \quad (14)$$

where $S^0_{nn^+}$ is the recombination velocity of the mino[rity] carrier at the n–n^+ junction under the dark conditio[n].

Using eqns (12) and (13) the carrier concentratio[n]

$X = w$, $p_n(w)$, can be written in terms of $p_n(0)$. The result is

$$p_n(w) = \frac{N_{DI}\gamma_0}{2k_0}\left[\sqrt{\left(1 + \frac{4k_0}{\gamma_0^2 N_{DI}} p_n(0)\right)} - 1\right] \quad (15)$$

where γ_0 and k_0 are separately defined as

$$\gamma_0 = \cosh\left(\frac{w}{L'_{pl}}\right) + k_0 \quad (16)$$

$$k_0 = \frac{S^0_{nn^+} L'_{pl}}{D'_{pl}} \sinh\left(\frac{w}{L'_{pl}}\right). \quad (17)$$

The carrier concentration $p_n(0)$ can be written in terms of p–n junction voltage by using the charge neutrality condition and the pn product relation at $X = 0$, i.e. $p_n(0)[p_n(0) + N_{DI}] = n_{io}^2 \exp(qV_J/k_BT)$:

$$p_n(0) = \frac{N_{DI}}{2}\left[\sqrt{\left(1 + \left(\frac{2n_{io}}{N_{DI}}\right)^2 \exp\left(\frac{qV_J}{k_BT}\right)\right)} - 1\right]. \quad (18)$$

Combining eqns (15) and (18) the carrier concentration at $X = w$, $p_n(w)$, may be rewritten as

$$p_n(w) = \frac{N_{DI}\gamma_0}{2k_0}\left\{\sqrt{\left(1 + \frac{2k_0}{\gamma_0^2}\left[\sqrt{\left(1 + \left(\frac{2n_{io}}{N_{DI}}\right)^2 \times \exp\left(\frac{qV_J}{k_BT}\right)\right)} - 1\right]\right)} - 1\right\}. \quad (19)$$

For the p^+–n–n^+ BSF solar cell shown in Fig. 1, the open-circuit voltage V_{oc} is the p^+–n junction voltage V_J plus the voltage developed across the low concentration base region, V_B, and plus the voltage developed across the high-low junction, V_{JB}. Combining eqns (6), (11), (19), the open-circuit voltage for the p^+–n–n^+ solar cell may be written as:

$$V_{oc} = V_J + V_{JB} + V_B \quad \text{for } p^+\text{–}n\text{–}n^+ \quad (20)$$

$$V_{JB} = \frac{k_BT}{q}\ln\left\{1 + \frac{\gamma_0}{k_0}\left[\sqrt{\left(1 + \frac{2k_0}{\gamma_0^2}\left[\sqrt{\left(1 + \left(\frac{2n_{io}}{N_{DI}}\right) \times \exp\left(\frac{qV_J}{k_BT}\right)\right)} - 1\right]\right)} - 1\right]\right\} \quad (21)$$

$$V_B = \frac{k_BT}{q}\left(\frac{b-1}{b+1}\right)\left\{\frac{\sqrt{\left(1 + \left(\frac{2n_{io}}{N_{DI}}\right)^2 \exp\left(\frac{qV_J}{k_BT}\right)\right)} + \left(\frac{b-1}{b+1}\right)}{\frac{\gamma_0}{k_0}\left[\sqrt{\left(1 + \frac{2k_0}{\gamma_0^2}\left[\sqrt{\left(1 + \left(\frac{2n_{io}}{N_{DI}}\right)^2 \exp\left(\frac{qV_J}{k_BT}\right)\right)} - 1\right]\right)} - 1\right] + \frac{2b}{b+1}}\right\}. \quad (22)$$

The analytical developments of V_B, V_{JB} for the n^+–p–p^+ BSF solar cell proceed analogously to those of the p^+–n–n^+ solar cell, except that the open-circuit voltage of the n^+–p–p^+ BSF solar cell is the n^+–p junction voltage V_J plus the voltage developed across the high-low junction, V_{JB}, and minus the voltage developed across the low-concentration base region, V_B. The results are:

$$V_{oc} = V_J + V_{JB} - V_B \quad \text{for } n^+\text{–}p\text{–}p^+ \quad (23)$$

$$V_{JB} = \frac{k_BT}{q}\ln\left\{1 + \frac{\gamma_1}{2k_1}\left[\sqrt{\left(1 + \frac{2k_1}{\gamma_1^2}\left[\sqrt{\left(1 + \left(\frac{2n_{io}}{N_{AI}}\right)^2 \times \exp\left(\frac{qV_J}{k_BT}\right)\right)} - 1\right]\right)} - 1\right]\right\} \quad (24)$$

$$V_B = \frac{k_BT}{q}\left(\frac{b-1}{b+1}\right)\ln\left\{\frac{\sqrt{\left(1 + \left(\frac{2n_{io}}{N_{AI}}\right)^2 \exp\left(\frac{qV_J}{k_BT}\right)\right)} - \left(\frac{b-1}{b+1}\right)}{\frac{\gamma_1}{k_1}\left[\sqrt{1 + \frac{2k_1}{\gamma_1^2}\left[\sqrt{\left(1 + \left(\frac{2n_{io}}{N_{AI}}\right)^2 \exp\left(\frac{qV_T}{k_BT}\right)\right)} - 1\right]} - 1\right] + \frac{2}{b+1}}\right\} \quad (25)$$

where γ_1 and k_1 are separately defined as

$$\gamma_1 = \cosh\left(\frac{w}{L'_{nl}}\right) + k_1 \quad (26)$$

$$k_1 = \frac{S^0_{pp^+} L'_{nl}}{D'_{nl}} \sinh\left(\frac{w}{L'_{nl}}\right) \quad (27)$$

$$S^0_{pp^+} = \frac{N_{AI} D_{nh}}{N_{Ah} L_{nh}} \exp\left(\frac{\Delta E_{G1}}{k_BT}\right) \coth\left(\frac{\Delta w_1}{L_{nh}}\right). \quad (28)$$

Note that $S^0_{pp^+}$ and $S^0_{nn^+}$ are calculated by assuming the infinite surface recombination velocity at the back-side contact. Note again that eqns (20)–(25) are exact, and are valid for both the low- and high-levels of optical illumination.

3. THE CORRELATION BETWEEN THE OPEN-CIRCUIT VOLTAGE AND THE SHORT-CIRCUIT CURRENT

To relate the junction voltage V_J to the illumination level, the continuity equations, in general, must be solved. However, the continuity equation is linear for both the low- and high-level injections. Without the detailed calculations, the total current flowing across the p–n junction is known to be consisted of two major components: the dark current density and the optical

generation current. For first order approximation, the principle of superposition is assumed to be valid for J_t, then we obtain

$$j_t = j_t\Big|_{\substack{G^0=0\\V_j\neq 0}} + j_t\Big|_{\substack{G^0\neq 0\\V_j=0}}. \tag{29}$$

The first term of eqn (29) is defined as the current density of zero net optical generation rate ($G_0 = 0$), which is known to be equivalent to the dark current flowing across the dark diode, i.e.

$$j_D = j_t\Big|_{\substack{G^0=0\\V_j\neq 0}} = -j_{do}\exp\left(\frac{qV_J}{k_BT}\right) \tag{30}$$

where j_{do} is the saturated dark current of the dark diode in the BSF solar cell.

The second term of eqn (29) is defined as the current density of $V_j = 0$ and $G^0 \neq 0$, which is known to be equivalent to the conventional short-circuit current across the solar cell, i.e.

$$J_{sc} = j_t\Big|_{\substack{G^0\neq 0\\V_j=0}}. \tag{31}$$

Substituting eqns (30) and (31) into (29), the resultant current density is similar to that of the classical relation, i.e.

$$J_t = J_D + J_{sc} = -J_{do}\exp\left(\frac{qV_J}{k_BT}\right) + J_{sc}. \tag{32}$$

For open-circuit condition, $J_t = 0$, eqn (32) gives

$$V_j = \frac{k_BT}{q}\ln\left(\frac{J_{sc}}{J_{do}}\right). \tag{33}$$

Now, let us proceed the identification of J_{do}. In the case of the p^+–n–n^+ diode, the saturated dark current consists of two components: the saturated electron current from the p^+ region to the n–n^+ region, $J_{do,n}$; the saturated hole current from the n–n^+ region to the p^+ region, $J_{do,p}$, which can be separately written as

$$j_{do,n} = q\frac{D_{nE}}{L_{nE}}\frac{n_{io}^2}{N_{AE}}\exp\left(\frac{\Delta E_{G2}}{k_BT}\right)\left\{\frac{\sinh\left(\frac{\Delta w_2}{L_{nE}}\right) + \frac{S_{FC}L_{nE}}{D_{nE}}\cosh\left(\frac{\Delta w_2}{L_{nE}}\right)}{\cosh\left(\frac{\Delta w_2}{L_{nE}}\right) + \frac{S_{FC}L_{nE}}{D_{nE}}\sinh\left(\frac{\Delta w_2}{L_{nE}}\right)}\right\} \tag{34}$$

$$j_{do,p} = q\frac{D_{pl}}{L_{pl}}\frac{n_{io}^2}{N_{Dl}}\left\{\frac{\sinh\left(\frac{w}{L_{pl}}\right) + \frac{S_{nn^+}^0L_{pl}}{D_{pl}}\cosh\left(\frac{w}{L_{pl}}\right)}{\cosh\left(\frac{w}{L_{pl}}\right) + \frac{S_{nn^+}^0L_{pl}}{D_{pl}}\sinh\left(\frac{w}{L_{pl}}\right)}\right\} \tag{35}$$

where N_{AE} is the front p^+-region concentration; ΔE_{G2} is the magnitude of the energy-gap shrinkage in the front p^+-region; S_{FC} is the recombination velocity for electrons at the front metal contact; D_{nE} and L_{nE} are the diffusivity and the diffusion length for electrons in the front p^+-region, respectively. Note that $j_{do} = j_{do,n} + j_{do,p}$.

Similar expressions of the saturated dark current components can be easily written for the n^+–p–p^+ solar cell. Substituting eqn (33) into eqns (20)–(22), the complete expression for the open-circuit voltage of the p^+–n–n^+ solar cell may be written as

$$V_{oc} = \frac{k_BT}{q}\ln\left\{\frac{J_{sc}}{J_{do}}\left[1 + \frac{\gamma_0}{2k_0}\left(\sqrt{\left(1 + \frac{2k_0}{\gamma_0^2}\left[\sqrt{\left(1+\left(\frac{2n_{io}}{N_{Dl}}\right)^2\left(\frac{J_{sc}}{J_{do}}\right)\right)} - 1\right]\right)} - 1\right)\right]\right\}$$
$$+ \frac{k_BT}{q}\left(\frac{b-1}{b+1}\right)\left\{\frac{\sqrt{\left(1+\left(\frac{2n_{io}}{N_{Dl}}\right)^2\left(\frac{J_{sc}}{J_{do}}\right)\right)} + \frac{b-1}{b+1}}{\frac{\gamma_0}{k_0}\left[\sqrt{\left(1+\frac{2k_0}{\gamma_0^2}\left[\sqrt{\left(1+\left(\frac{2n_{io}}{N_{Dl}}\right)^2\left(\frac{J_{sc}}{J_{do}}\right)\right)}-1\right]\right)}-1\right] + \frac{2b}{b+1}}\right\}$$
$$\text{for } p^+\text{–}n\text{–}n^+ \tag{36}$$

Similarly, the complete expression for the open-circuit voltage of the n^+–p–p^+ solar cell is

$$V_{oc} = \frac{k_BT}{q}\ln\left\{\frac{J_{sc}}{J'_{do}}\left[1 + \frac{\gamma_1}{2k_1}\times\left(\sqrt{\left(1 + \frac{2k_1}{\gamma_1^2}\left[\sqrt{\left(1+\left(\frac{2n_{io}}{N_{Al}}\right)^2\left(\frac{J_{sc}}{J'_{do}}\right)\right)} - 1\right]\right)} - 1\right)\right\}$$
$$+ \frac{k_BT}{q}\left(\frac{b-1}{b+1}\right)\times\left\{\frac{\sqrt{\left(1+\left(\frac{2n_{io}}{N_{AL}}\right)^2\left(\frac{J_{sc}}{J'_{do}}\right)\right)} - \left(\frac{b-1}{b+1}\right)}{\frac{\gamma_1}{k_1}\left[\sqrt{\left(1+\frac{2k_1}{\gamma_1^2}\left[\sqrt{\left(1+\left(\frac{2n_{io}}{N_{AL}}\right)^2\left(\frac{J_{sc}}{J'_{do}}\right)\right)}-1\right]\right)}-1\right] + \frac{2}{b+1}}\right\}$$
$$\text{for } n^+\text{–}p\text{–}p^+ \tag{37}$$

where J'_{do} is the saturated dark current of the dark diode in the n^+–p–p^+ solar cell, which consists of two components, is similar to that of the p^+–n–n^+ solar cell.

4. NUMERICAL RESULTS AND COMPARISONS

In order to compare the derived results with the exact numerical analysis of Fossum *et al.*[4], the minority carrier diffusivities as the function of the base impurity concentration, adopted by the original paper of Fossum[7], are separately expressed as follows:

$$D_n = \frac{D_{no}}{\left[1 + \frac{81N_A}{N_A + 3.2\times 10^{18}\,\text{cm}^{-3}}\right]^{1/2}} \tag{38}$$

$$D_p = \frac{D_{po}}{\left[1 + \frac{350 N_D}{N_D + 1.05 \times 10^{19}\,\text{cm}^{-3}}\right]^{1/2}} \qquad (39)$$

$qD_{no} = \mu_{no} k_B T$ ($\mu_{no} = 1350\,\text{cm}^2/\text{v}\cdot\text{sec}$ for $T =$ ...); $qD_{po} = \mu_{po} k_B T$ ($\mu_{po} = 480\,\text{cm}^2/\text{v}\cdot\text{sec}$ for $T =$ ...). Note that eqns (38) and (39) are used in both the ...nd high-concentration regions of BSF solar cells. ...ptimistic minority carrier life time, adopted by ...m[5] is used for both electrons and holes, which is ...ssed by

$$\tau_n = \tau_p = \frac{3.95 \times 10^{-4} S}{1 + \frac{N}{7.1 \times 10^{15}\,\text{cm}^{-3}}} \qquad (40)$$

...re τ_n and τ_p are the minority carrier life times of ...ons and holes, respectively; N is the doping con...tration with $N = N_A$ for p-type semiconductor, and $= N_D$ for n-type semiconductor. In general, the ...rity carrier diffusion length of the dark diode can be ...ined by the known relations, i.e. $L_p = \sqrt{(D_p \tau_p)}$ for ...s; $L_n = \sqrt{(D_n \tau_n)}$ for electrons. However, the ...ctive minority carrier diffusion length and diffusivity ...er the high-levels of optical illumination (shown in ... 12) will be different. For example: for the case of ...p^+–n–n^+ BSF solar cell operated under high-level ...mination condition, $L'_{pl} = \sqrt{(2)} L_{pl}$, $D'_{pl} = 2D_{pl}$; ...ereas under low-level illumination condition, $L'_{pl} =$ ..., $D'_{pl} = D_{pl}$. Similarly, for the case of the n^+–p–p^+ ...F solar cell operated under high-level illumination ...dition, $L'_{nl} = \sqrt{(2)} L_{nl}$, $D'_{nl} = 2D_{nl}$; whereas under ...-level illumination condition, $L'_{nl} = L_{nl}$, $D'_{nl} = D_{nl}$.

...For the cases of the n^+–p–p^+ and p^+–n–n^+ solar cells ...erated at room temperature and with the same base ...ping concentration of $N_{Al} = N_{Dl} = 1.2 \times 10^{15}\,\text{cm}^{-3}$, the parameters used for numerical calculations are shown in Table 1. Comparisons of the derived results (eqns 36 and 37) with those of the exact numerical analysis of Fossum *et al.*[3, 4] are shown in Fig. 2 where two surface recombination velocities of the front contact are cited. It is shown that excellent agreements between the present analytical results and the exact computer-aided numerical analysis of Fossum *et al.* are obtained for both n^+–p–p^+ and p^+–n–n^+ BSF solar cells with the front contact surface recombination velocity of 10^5 cm/sec which is also used in the exact numerical analysis of Fossum[5]. In order to clarify the physical pictures of the BSF solar cells shown in Fig. 2, the dark current components of the dark diode and the voltage components of the open-circuit voltage for both the p^+–n–n^+ and n^+–p–p^+ BSF solar cells are listed in Table 2 and Table 3 where the surface recombination velocity of the front contact is 10^5 cm/sec. For the data of the p^+–n–n^+ BSF solar cell shown in Table 2, the dark current component $J_{do,n}$ of the p^+–n–n^+ solar cell is comparable to that of $J_{do,p}$, which means that the minimization of $J_{do,n}$ is still needed. If the doping concentration (N_{AE}) and width (Δw_2) of the emitter region are optimized for the pass of the light spectrum and the consideration of contact resistance, then $J_{do,n}$ will be fixed; the minimization of $J_{do,p}$ may be obtained by further lowering the doping concentration of the low concentration base region to $10^{14}/\text{cm}^3$, and increasing the doping concentration of the high concentration base region to $5 \times 10^{19}/\text{cm}^3$, if the dimensions of the present p^+–n–n^+ solar cell does not change. For the data of the n^+–p–p^+ solar cell shown in Table 3, the dark current component $J'_{do,p}$ is about ten times larger than that of $J'_{do,n}$, which means that the high-low junction (p–p^+) in the present case does not give the efficient suppression of the minority carrier injected from the emitter n^+-

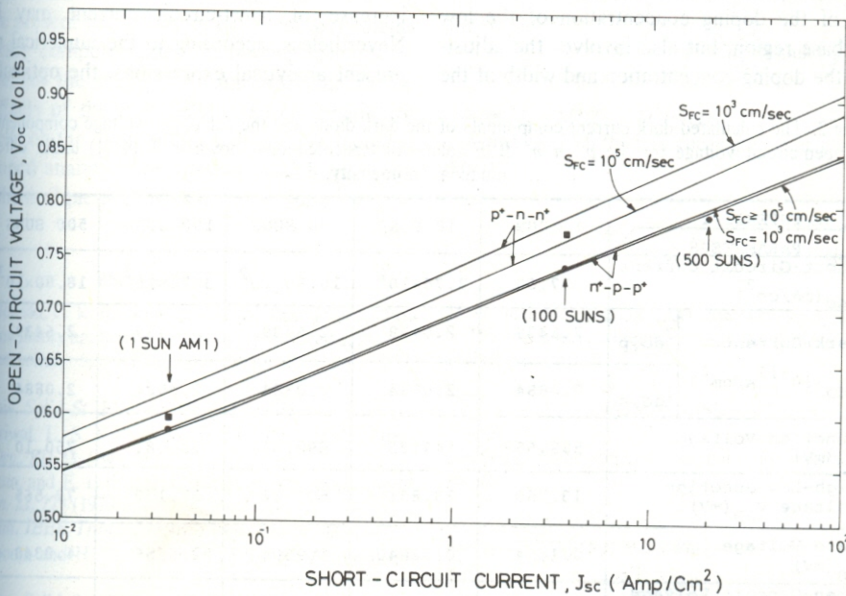

Fig. 2. Open-circuit voltage vs short-circuit current for p^+–n–n^+ and n^+–p–p^+ silicon solar cells. The points were obtained from the exact computer-sided analysis of Fossum *et al.* (Ref. [4, 5]); the solid lines are the numerical results of the present theory with all parameters shown in Table 1.

Table 1. Parameters ($T = 300°K$) of silicon BSF solar cells used for numerical calculations.

Parameter	Value
Front $p^+(n^+)$ region thickness (Δw_2)	$\Delta w_2 = 0.25$ μm
Front $p^+(n^+)$ region concentration, $N_{AE}(N_{DE})$	$N_{AE}=N_{DE}=2\times10^{20}/cm^3$
Back $n^+(p^+)$ region thickness (Δw_1)	$\Delta w_1 = 0.5$ μm
Back $n^+(p^+)$ region concentration, $N_{Dh}(N_{Ah})$	$N_{Dh}=N_{Ah}=10^{19}/cm^3$
Base region concentration, $N_{D\ell}(N_{A\ell})$	$N_{D\ell}=N_{A\ell}=1.2\times10^{15}/cm^3$
Base region thickness (w)	w = 150 μm
Surface recombination velocity of back contact (S_{bc})	$S_{bc} = \infty$
Surface recombination velocity of front contact (S_{FC})	$S_{FC}=10^3$cm/sec, 10^5cm/sec
Minority carrier diffusion length at front $p^+(n^+)$ region, $L_{nE}(L_{pE})$	$L_{pE}=0.9$μm ($L_{nE}=2.3$μm)
Minority carrier diffusion length at n(p) base region, $L_{p\ell}(L_{n\ell})$	$L_{n\ell}=1078.4$μm ($L_{p\ell}=641.49$μm)
Minority carrier diffusion length at back $n^+(p^+)$ region, $L_{ph}(L_{nh})$	$L_{nh}=11.142$μm ($L_{ph}=5.1537$μm)
Minority carrier diffusivity at front $p^+(n^+)$ region, $D_{nE}(D_{pE})$	$D_{pE}=0.68cm^2/sec$ ($D_{nE}=3.8882$ cm^2/sec)
Minority carrier diffusivity at n(p) base region, $D_{p\ell}(D_{n\ell})$	$D_{n\ell}=34.419cm^2/sec$ ($D_{p\ell}=$ $12.179cm^2/sec$)
Minority carrier diffusivity at back $n^+(p^+)$ region, $D_{ph}(D_{nh})$	$D_{nh}=4.4299cm^2/sec$ ($D_{ph}=$ $0.94776cm^2/sec$)

region into the p-p^+ region. Similarly, if the doping concentration (N_{DE}) and width (Δw_2) of the emitter region is assumed to be fixed for the same reason stated above, then the minimization of $J'_{do,p}$ not only involves the reduction of the doping concentration of the low concentration base region, but also involves the adjustments of both the doping concentration and width of the high concentration base region, which is quite co[m]plicated and will be discussed elsewhere[8]. Note th[at] the increase of the base width (w), in general, w[ill] decrease the open-circuit voltage, although the s[light] increase of short-circuit current may be obtaine[d]. Nevertheless, according to the numerical results of t[he] present analytical expressions, the optimal doping co[ncentration]

Table 2. The calculated dark current components of the dark diode and the calculated voltage components of the open-circuit voltage for the p^+-n-n^+ BSF solar cell (specifications shown in Table 1) under different illumination intensity.

PARAMETERS \ INTENSITY		1 SUN	10 SUNS	50 SUNS	100 SUNS	500 SUNS
Short-Circuit Current J_{sc} (mA/cm^2)		37.60	3.76×10^2	18.80×10^2	3.76×10^3	18.80×10^3
Dark Current J_{do} ($10^{-12}A/cm^2$)	$J_{do,p}$	2.6439	2.6439	2.6439	2.6439	2.6439
	$J_{do,n}$*	2.0884	2.0884	2.0884	2.0884	2.0884
Junction Voltage V_J (mV)		589.65	649.23	690.51	708.81	750.10
High-Low Junction Voltage V_{JB} (mV)		13.260	33.801	50.022	57.159	72.565
Base Voltage V_B (mV)		0.1404	0.82640	1.9504	2.6656	4.8340
Open-Circuit Voltage V_{oc} (mV)		602.91	683.03	740.53	768.63	827.50

* $S_{FC} = 10^5$cm/sec

Table 3. The calculated dark current components of the dark diode and the calculated voltage components of the open-circuit voltage for the n^+–p–p^+ BSF solar cell (specifications shown in Table 1) under different illumination intensity.

INTENSITY / PARAMETERS		1 SUN	10 SUNS	50 SUNS	100 SUNS	500 SUNS
Short-Circuit Current J_{sc} (mA/cm^2)		37.60	3.76×10^2	18.80×10^2	3.76×10^3	18.80×10^3
Dark Current J'_{do} (10^{-12}A/cm^2)	$J'_{do,n}$	7.8155	7.8155	7.8155	7.8155	7.8155
	$J'_{do,p}$ *	0.74492	0.74492	0.74492	0.94492	0.74492
Junction Voltage V_J (mV)		574.23	633.83	672.45	693.48	734.76
High-Low Junction Voltage V_{JB} (mV)		9.270	27.367	42.646	49.432	64.196
Base Voltage V_B (mV)		0.1975	1.0475	2.3320	3.1260	5.4656
Open-Circuit Voltage V_{oc} (mV)		583.30	660.15	712.764	739.79	730.49

* $S_{FC} = 10^5$ cm/sec

entration and width of the high concentration base region is found to be $\Delta w_1 = 5\,\mu m$, $N_{Dh} = N_{Ah} = 1\times10^{18}/cm^3$.

It should be emphasized again that the high-low junction voltage V_{JB} and the base region voltage V_B may not be neglected, especially for high-levels of optical illumination.

5. CONCLUSIONS

Based on more realistic assumptions and boundary conditions, the accurate analytical expressions of the open-circuit voltages for the n^+–p–p^+ and p^+–n–n^+ BSF solar cells are derived in terms of the short circuit current density and the known saturated dark current density of the dark diode. Using the same device parameters as stated by Fossum *et al.*, the numerical results of the present theory are in excellent agreements with the exact computer-aided numerical analysis of Fossum *et al.* for the range of 1 sun (AM1) up to 500 suns. The effects of the resistivities and dimensions of BSF solar cells on the open-circuit voltages are included in the developed analytical expressions which may give more clear physical pictures of BSF solar cells.

REFERENCES

1. M. P. Godlewski, C. R. Baraona, and H. W. Brandhorst, "Low high junction theory applied to solar cells", presented at the 10th IEEE *Photovoltaic Specialist Conf.*, Palo Alto, CA, 13–15 (1973).
2. A. G. Sabnis, *Solid-St. Electron.* **21**, 581 (1978).
3. S. R. Dhariwal, L. S. Kothari, and S. C. Jain, *IEEE Trans. Electron Dev.*, **ED-23**, 504 (1976).
4. J. G. Fossum, and E. L. Burgess, and F. A. Lindholm, *Solid-St. Electron.* **21**, 729 (1978).
5. J. G. Fossum, *IEEE Trans. Electron Dev.*, **ED-24**, 322 (1977).
6. J. W. Slotboom and H. C. De Graaff, *Solid-St. Electron.* **19**, 857 (1976).
7. J. G. Fossum, *Solid-St. Electron.* **19**, 504 (1976).
8. Ching-Yuan Wu and Wen-Zen Shen to be published elsewhere.

APPENDIX

In deriving eqn (12), the current density for holes can be written as the following standard form:

$$j_p(x) = -\xi q D_{pl}\frac{\partial p_n(x)}{\partial x} \tag{A1}$$

where $\xi = 1$ for low-levels of optical illumination; $\xi = 2$ for high-levels of optical illumination.

Combining eqn (A1) and eqn (4), and assuming low generation rate in the neutral base region, the hole density distribution in the neutral base region can be easily calculated by using the following boundary condition, i.e.,

$$-\xi D_{pl}\frac{\partial[p_n(x)-p_{no}]}{\partial x} + S_{nn^+}[p_n(w)-p_{no}] = 0, \tag{A2}$$

the result is

$$p_n(x)-p_{no} = \left\{\frac{\cosh\left(\frac{w-x}{L'_{pl}}\right)+\frac{S_{nn^+}L'_{pl}}{D'_{pl}}\sinh\left(\frac{w-x}{L'_{pl}}\right)}{\cosh\left(\frac{w}{L'_{pl}}\right)+\frac{S_{nn^+}L'_{pl}}{D'_{pl}}\sinh\left(\frac{w}{L'_{pl}}\right)}\right\}[p_n(0)-p_{no}] \tag{A3}$$

where $L'_{pl} = \sqrt{(\xi D_{pl})}$, $D'_{pl} = \xi D_{pl}$.

Using eqn (A3) the hole concentration at $x = w$ can be expressed by

$$p_n(w)-p_{no} = \frac{(p_n(0)-p_{no})}{\cosh\left(\frac{w}{L'_{pl}}\right)+\frac{S_{nn^+}L'_{pl}}{D_{pl}}\sinh\left(\frac{w}{L'_{pl}}\right)} \tag{A4}$$

If we neglect p_{no} in eqn (A4), eqn (12) can be obtained.

The surface recombination velocity of the n–n^+ junction, S_{nn^+}, is defined as

$$j_{sub} + qS_{nn^+}[p_n(w)-p_{no}] = 0 \tag{A5}$$

where j_{sub} is the substrate current density, which can be expressed by

$$j_{sub} = -\frac{qD_{ph}}{L_{ph}}[p_n(w+w_{sc})-p_{no}]\left\{\frac{\sinh\left(\frac{\Delta w_1}{L_{ph}}\right)+\frac{S_{bc}L_{ph}}{D_{ph}}\cosh\left(\frac{\Delta w_1}{L_{ph}}\right)}{\cosh\left(\frac{\Delta w_1}{L_{ph}}\right)+\frac{S_{bc}L_{ph}}{D_{ph}}\sinh\left(\frac{\Delta w_1}{L_{ph}}\right)}\right\}. \tag{A6}$$

Combining eqns (A6) and (A5), the surface recombination velocity of the $n - n^+$ junction may be expressed by

$$S_{nn^+} \cong \frac{D_{ph}}{L_{ph}} \frac{p_n{}^+(w + w_{sc})}{p_N(w)} \left\{ \frac{\sinh\left(\frac{\Delta w_1}{L_{ph}}\right) + \frac{S_{bc}L_{ph}}{D_{ph}} \cosh\left(\frac{\Delta w_1}{L_{ph}}\right)}{\cosh\left(\frac{\Delta w_1}{L_{ph}}\right) + \frac{S_{bc}L_{ph}}{D_{ph}} \sinh\left(\frac{\Delta w_1}{L_{ph}}\right)} \right\}. \quad \text{(A7)}$$

Using eqns (7), (9), (10), eqn (A7) can be rewritten as

$$S_{nn^+} = \frac{D_{ph}N_{pl}}{L_{ph}N_{Dh}} \exp\left(\frac{\Delta E_{G1}}{k_B T}\right) \left(1 + \frac{p_n(w)}{N_{Dl}}\right) \left\{ \frac{\sinh\left(\frac{\Delta w_1}{L_{ph}}\right) + \frac{S_{bc}L_{ph}}{D_{ph}} \cosh\left(\frac{\Delta w_1}{L_{ph}}\right)}{\cosh\left(\frac{\Delta w_1}{L_{ph}}\right) + \frac{S_{bc}L_{ph}}{D_{ph}} \sinh\left(\frac{\Delta w_1}{L_{ph}}\right)} \right\}. \quad \text{(A8)}$$

If the surface recombination velocity of the back contact is assumed to be an infinite, then eqn (A8) can be reduced to eqns (13) and (14) in the text.